BWF Sports Science Research Project 2019-2020

Final Report

August 2020

Title: Towards Intelligent Monitoring of Lower Extremity Loadings in Badminton from Lab to on-Court Analysis

Area: Biomechanics/Sports Medicine & Injuries

Researcher: Dr. Qichang Mei*; A/Prof. Justin Fernandez; Prof. Yaodong Gu

Email: qmei907@aucklanduni.ac.nz

Affiliations: Ningbo University (China); The University of Auckland (New Zealand)

Project Summary

This project was aimed to investigate, estimate, and monitor the knee and ankle joint loadings of badminton athletes from lab test with 'gold-standard' facilities to on-court intelligent analysis. Previously established protocol of motion capture and musculoskeletal modelling techniques were employed, with further integration of wearable IMUs (inertial magnetic unit). We also developed Principal Component Analysis (PCA) model to extract features in the loading parameters, and multivariate Partial Least Square Regression (PLSR) machine learning model to correlate easily-collected variables, such as the approaching velocity, and peak acceleration, with knee and ankle loading parameters (moments and contact forces). Promising accuracy of the PLSR model using the input parameters was observed, further sensitivity analysis found a single variable from ankle IMU could predict an acceptable range of patterns and magnitudes of knee and ankle loadings. The attachment of this single IMU sensor could not only record and predict loading accumulation and distribution but also exert little influence on the movement of the lower extremity. Information from this project would be used to monitor lower extremity loading from badminton during training and competition sessions, and assist the training scheme design and dynamic adjustment in a scientific manner, thus help prevent fatigue, reduce injury risks and improve training efficacy and athletic performance. ***(We also attached the PCA and PLSR models developed from this project in the Appendix for the reference of research interest from the badminton research or practitioner communities.)***

1. Background / Introduction

The current project followed up our previous project on the investigation of knee joint loadings during directional badminton lunges using musculoskeletal and finite element modelling, which was supported by the BWF research project 2018-2019. The project found that the left-side (forecourt and backcourt) backhand lunges exhibited larger knee loadings (i.e. joint moments and contact forces) comparing to the right-side (forecourt and backcourt) forehand lunges [*ref to Mei et al., BWF project report 2018-2019, (2019)*]. It was further proposed that a next-step research focusing on the dynamic monitoring of lower extremity loadings from the lab-simulated court towards on-court intelligent monitoring. A key issue in previous studies was that the lab-simulated studies strictly controlled variables, which is not the case during

the on-court real scenario training and competition.

The injuries to the lower extremity, especially knee and ankle joints, have been commonly reported and documented in previous studies (Chard & Lachmann, 1987; Fahlström et al., 1998; Fong et al., 2007; Jérgensen & Winge, 1987; Kroner et al., 1990). Lab-simulated experiments have been conducted to reveal the potential injury mechanism (W. Lam et al., 2020; Lee & Loh, 2019; Phomsoupha & Laffaye, 2020). However, it was also acknowledged that biomechanical experiments in the lab-simulated environment are different from on-court 'real scenario' training and competition.

The prevention of injuries in badminton has been a key research interest of several area across sports scientist, biomechanist, physical therapist and sport medicine clinician. Based on the contributing mechanism, the injuries have been classified as chronic injury due to the reason of repetitive loading accumulation and acute injury from unexpected incursion (Goh et al., 2013; Reeves et al., 2015). Our recent study (Mei et al., 2020) has revealed the loading patterns of knee joint from directional sub- and maximal- lunges in a lab-simulated court. The challenge of discrepancy between lab test with on-court situation was further reported and highlighted. Recently, the rapidly emerging wearable technology in the biomechanics research community provide plausible and accessible approaches to solve this issue with integration of machine learning and artificial intelligence techniques. These have been implemented in the measurement of gait patterns (Shahabpoor & Pavic, 2017) and monitoring of running loads accumulation (Ueberschär et al., 2019; Van Hooren et al., 2020).

The purpose of the current project was to conduct a perspective study on monitoring of loads in the knee and ankle joints using wearable technology and machine learning estimation. Thus, this project firstly correlated the data from wearables with ground-truth lab test to develop and validate intelligent machine learning models. Specifically, the Principal Component Analysis (PCA) model will be developed for feature extraction and dimensionality reduction thus correlating data in wearables with 'ground-truth' lab test and the Partial Least Squares (PLS) regression machine learning model for multivariate correlation and prediction to estimate the loads in the 'real world' scenario on-court badminton training and competition.

2. Methodology

2.1 Participant

A total of 25 badminton athletes joint the lab test with synchronized collection of motion data and IMU (inertial measurement unit) data (fist session). Another 25 athletes participated the data collection during training or match during on-court real situation (second session). This study was approved by the ethic committee from the Research Academy of Grand Health in Ningbo University. All athletes were informed of the requirements, objectives and procedures of the lab and on-court tests with written consent.

2.2 Protocol

The first session of the lab test synchronized the 3D motion capture and wearable sensors. The test involved a twelve-camera Vicon system and Vicon IMU (inertial measurement unit) wearable sensors (Vicon Metrics Ltd., Oxford, United Kingdom), and AMTI 3D force plate (AMTI, Watertown, MA, United States) (**Figure 1**). The collection frequency of Vicon camera system was set at 200Hz, and the IMU and force plate were set at 1000Hz.

In order to mimic the real movements, we employed an established full-body marker-set model during motion capture (Rajagopal et al., 2016). The IMU sensors to the ankle and knee joints were illustrated in the **Figure 1B**. Specifically, 2cm below the medial condyle of proximal tibia was placed for the knee IMU, and 3 cm superior to the medial malleolus of distal tibia was place for the ankle IMU (Sheerin et al., 2020; Xiang et al., 2020). To follow-up our previous project, the four directional sub-maximal and maximal lunges were performed with synchronous collection of motion, ground reaction force, and IMU data for further processing and analysis. Specifically, the sub- and maximal- right-forward forehand lunges (***Sub-RF***, and ***Max-RF***), sub- and maximal- left-forward backhand lunges (***Sub-LF***, and ***Max-LF***), right-backward backhand sub- and maximal- lunges (***Sub-RB***, and ***Max-RB***) and left-backward backhand sub- and maximal- lunges (***Sub-LB***, and ***Max-RB***) were performed.

The second session was performed on a real-court while the athletes conducted badminton training or match with attached IMU to the knee and ankle as highlighted placement in the **Figure 1B**. IMU signals from a single training or competition session (approximately 2 hours) were collected with data stored 'on-board' in the memory disk in the sensor. The data were then extracted for further processing and analysis.

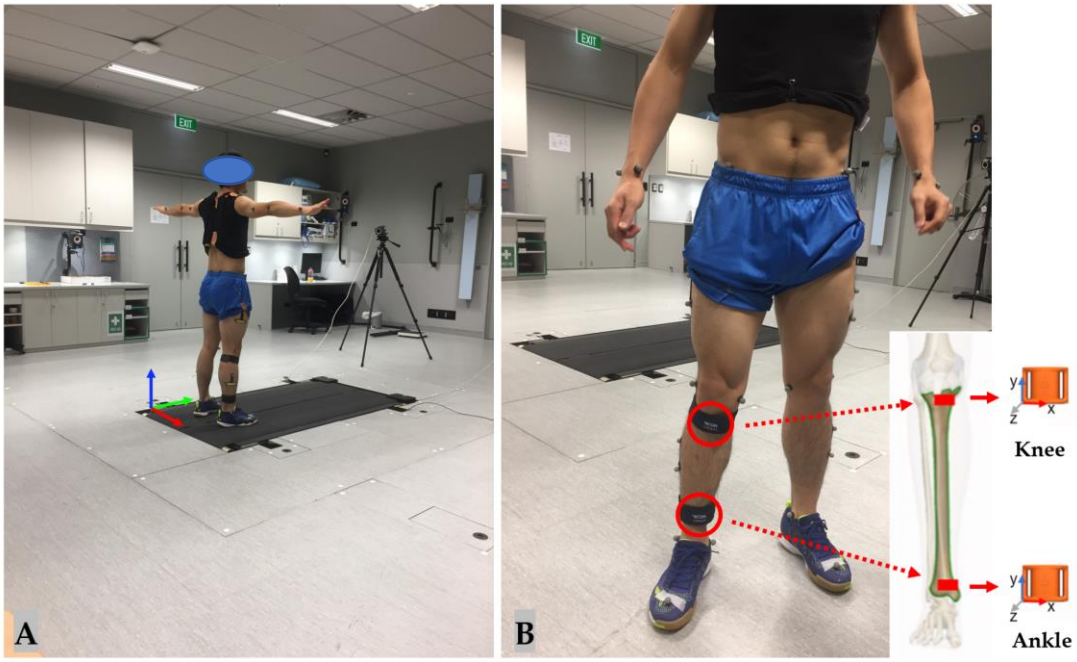

Figure 1. Illustration of lab setup and knee and ankle IMUs placement

2.3 Data Processing

Following previously established protocols of musculoskeletal OpenSim modelling, the joint kinematics, kinetics, and contact forces were calculated. Machine learning models were also developed and tested using motion capture data against the acceleration and angular velocity data from wearable sensors.

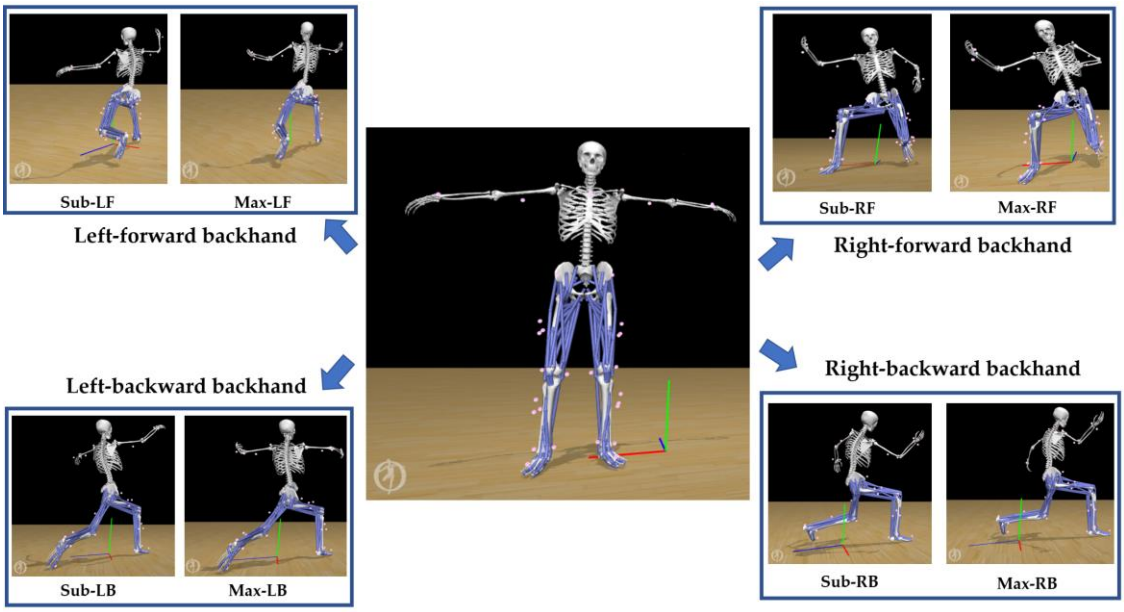

Figure 2. Illustration of musculoskeletal modelling pipeline

Firstly, the static marker positions and body mass were used to '**scale**' the generic model to athlete matching subject-specific musculoskeletal models (**Figure 2**) as per the standardized workflow (Delp et al., 2007). The '**Inverse kinematics**' (***IK***) algorithm, which minimized errors between virtual markers in the model and experimental marker trajectories, was employed to compute joint angles. Then the '***Inverse Dynamics***' (***ID***) was performed to calculate joints moment, and the '***Static Optimization***' (***SO***) was employed to compute muscle activation and forces. The estimated muscle activation was compared against measured surface EMG signals to validate the model. Lastly, the contact forces to the knee and ankle joints in the anterior/posterior (**x**), superior/inferior (**y**), and medial/lateral (**z**) directions were computed using '***Joint Reaction***' (***JR***) analysis.

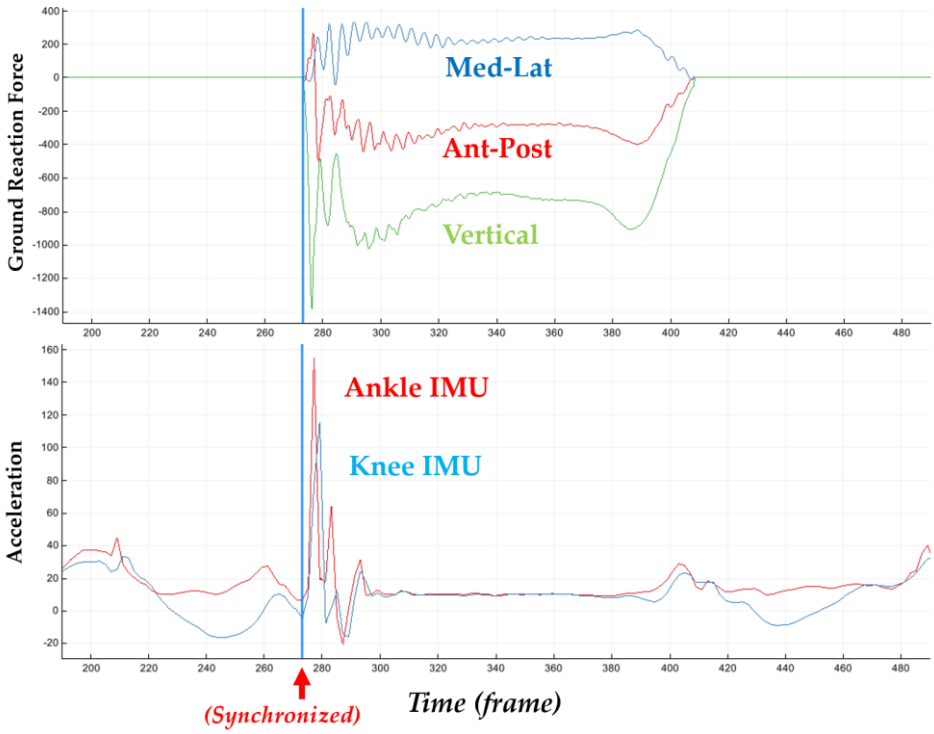

Figure 3. Illustration of synchronized IMU signals with ground reaction forces

Apart from the biomechanical variables, we also calculated the parameters of contact time, approaching velocity, peak IMU acceleration (**G**) in the knee and ankle joints as presented in the **Figure 3**. The axial (**y**-axis) acceleration of particular interest was taken for analysis to quantify the accumulation of impact in the lower extremity (tibia) (Rice et al., 2019; Tenforde et al., 2020), which was normalized by the gravitational acceleration (**G** = 9.8m/s^2).

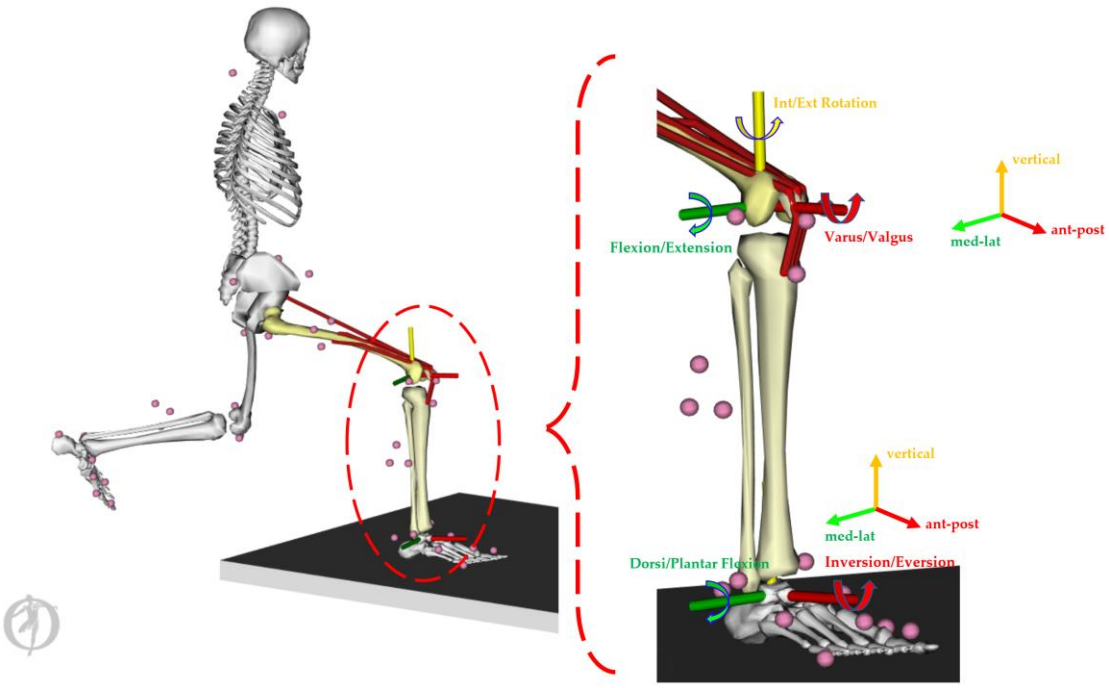

Figure 4. Illustration of knee and ankle loading parameters

The processed time-varying moment and contact force parameters during lunging stance (**Figure 4**), such as knee flexion/extension moment, knee varus/valgus moment, knee rotation moment, ankle dorsi/plantar flexion moment, ankle inversion/eversion moment, knee ant-post/med-lat/vertical contact forces, and ankle ant-post/med-lat/vertical contact forces were interpolated (normalized) into 101 datapoint for statistical modelling.

2.4 Statistical Modelling

We developed two multivariate statistical models in the current project, specifically Principal Component Analysis (PCA) model and Partial Least Squares Regression (PLSR) model. using the MATLAB software (R2019a, The MathWorks Inc., MA, USA).

The PCA multivariate technique was used to reduce the high-dimensional data matrices into orthogonal PCs (principal components), which explained major variations within the dataset (Deluzio et al., 1997; Lever et al., 2017). Each variation reported in the PCA modelling was feature extraction applied in the machine learning technique (Phinyomark et al., 2018).

Specifically as presented in the Equation **(1)**, the original matrices ($X = x^1, x^2, x^3, \ldots x^{99}, x^{100}, x^{101}$) * m were orthogonally transformed into uncorrelated principal components ($Z = z^1, z^2, z^3, \ldots, z^p$) ($p < 101$), corresponding loading vectors ($T^2 = T_1, T_2, T_3, \ldots T_m$) and residuals ($Q$), which was defined as $Z = X*T^2$ (Deluzio et al., 1997).

$$\begin{bmatrix} x_1^1 & x_1^2 & \cdots & x_1^{100} & x_1^{101} \\ \vdots & \vdots & \ddots & \vdots & \\ x_m^1 & x_m^2 & \cdots & x_m^{100} & x_m^{101} \end{bmatrix} = \begin{bmatrix} z_1^1 & z_1^2 & z_1^3 \\ \vdots & \vdots & \vdots \\ z_m^1 & z_m^2 & z_m^3 \end{bmatrix} \begin{matrix} T_1^2 & Q_1 \\ \vdots & \vdots \\ T_m^2 & Q_m \end{matrix} \qquad (1)$$

The m equals 200 (4*2*101 matrices) for PCA modelling of the four lunges (RF, LF, RB, and LB) with sub- and maximal- performance. This study mainly accounted for the main variations in the first three PCs (z^1, z^2, & z^3), which accounted for over 85~90% of variation. The variations in the vertical ground reaction force, knee and ankle moments, and contact forces of the first 3PCs were plotted against the mean for visualization of the key features, with '+' and '▽' representing upper and lower limits, respectively.

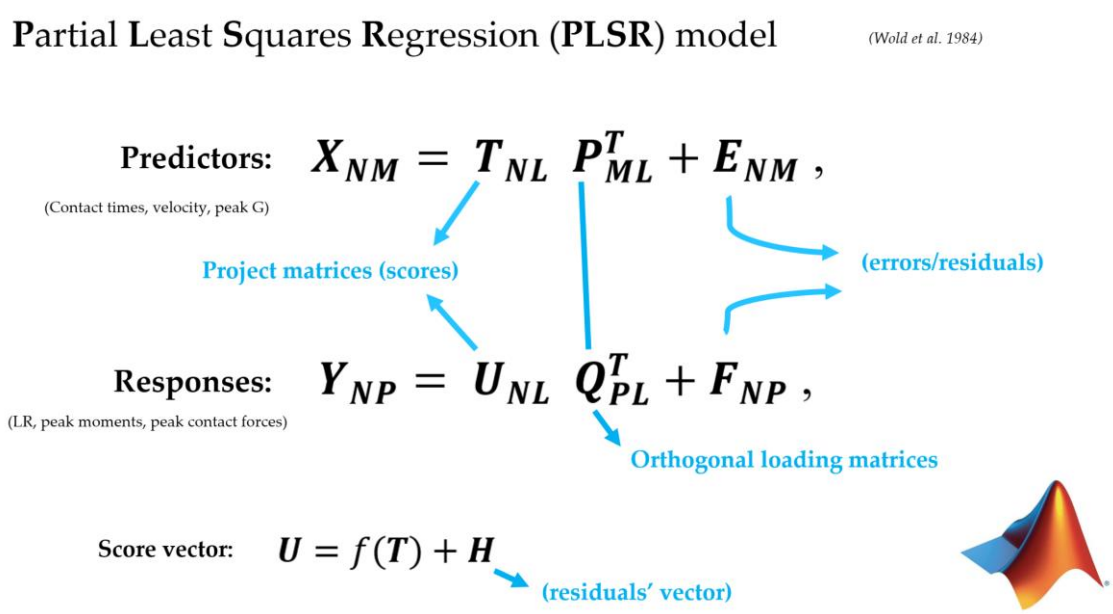

Figure 5. The development of PLSR machine learning

In terms of PLSR model, the two fundamental equations in PLSR are the predictor matrix ($\mathbf{X}_{NM}$) and the response matrix ($\mathbf{Y}_{NP}$) in the above **Figure 5**. The subscript N is the number of data sets (25*4 training samples in this study). The subscript M is the number of predictor variables (4 metrics, such as contact times, velocity, peak knee G, and peak ankle G). The subscript P is the number of response variables (12 loading variables, such as loading rate, knee flex-extension/varus-valgus/int-ext rotation moments, ankle dorsi-plantar flexion/ inversion-eversion moments, knee ant-post/med-lat/vertical contact forces, and ankle ant-post/med-lat/vertical contact forces), and the subscript L is the number of components. T and U are the projection matrices (also known as scores), and P and Q are the transposed orthogonal loading matrices (where the rows are created from eigenvectors or principal components), and E and F are the error or residual terms. The score vectors are related using a linear function, $U = f(T) + H$, where H is the vector of residuals.

3. Results / Key findings

3.1 PCA

The vertical ground reaction force (**Figure 6A**) was classified into four key phases, including initial impact peak, secondary impact peak, weight acceptance, and drive-off phases (**Figure 6B**). Following the PCA modelling of the vertical GRF, the first mode (**PC1, Figure 6C**) showed main variations from landing to the initial impact peak (Phase-**I**), which was loading rate (LR) being calculated as a key impact parameter. The second mode (**PC2, Figure 6D**) was in the secondary impact peak (Phase-**II**), and the third mode (**PC3, Figure 6E**) was the combination of variations in both initial and secondary impact peak (Phase-**I** & Phase-**II**).

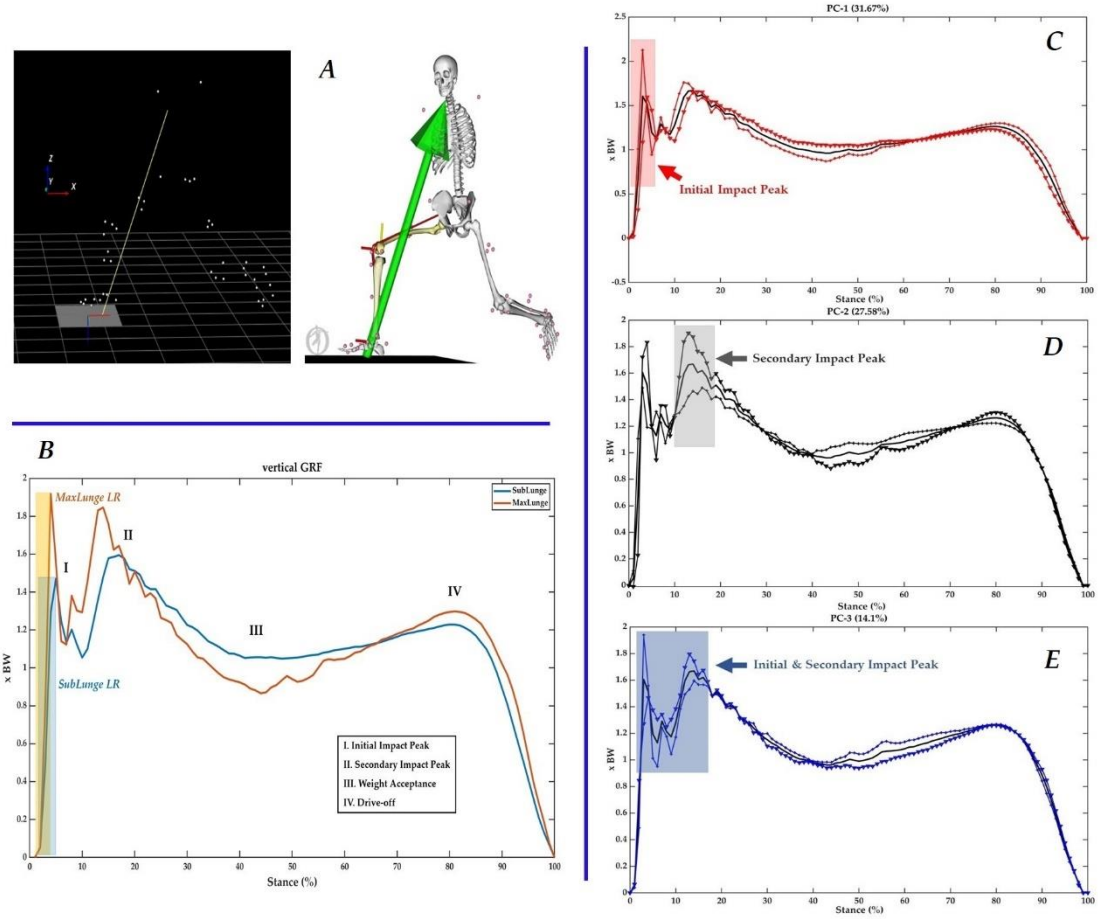

Figure 6. Classification of four phases in the lunging ground reaction force (**B**), and three principal modes of variance (**C, D & D**)

Consistent with the variations of vertical GRF, the knee flexion/extension and varus/valgus moments showed great variances during the landing (impact absorption) phase. As particular interest and principal mode to illustrate variance, the **PC1** of knee flexion/extension (33.96%) and varus/valgus (32.61%) moments are presented in the **Figure 7A & Figure 7B**. Similarly, the **PC1** of knee axial (vertical) contact force (**Figure 7D**) exhibited great variances during mid-stance (weight acceptance phase) with explanation of 35.26% between sub- and maximal- lunging steps.

Whilst the ankle dorsi/plantar flexion moments have variance over the stance, specifically the **PC1** (48.14%) during impact absorption and drive off phrases (**Figure 8A**). Similarly, in the axial contact force, a great variation (**PC1**, 40.22%) in the impact peaks (initial & secondary) and drive off phases was observed (**Figure 8B & Figure 8C**).

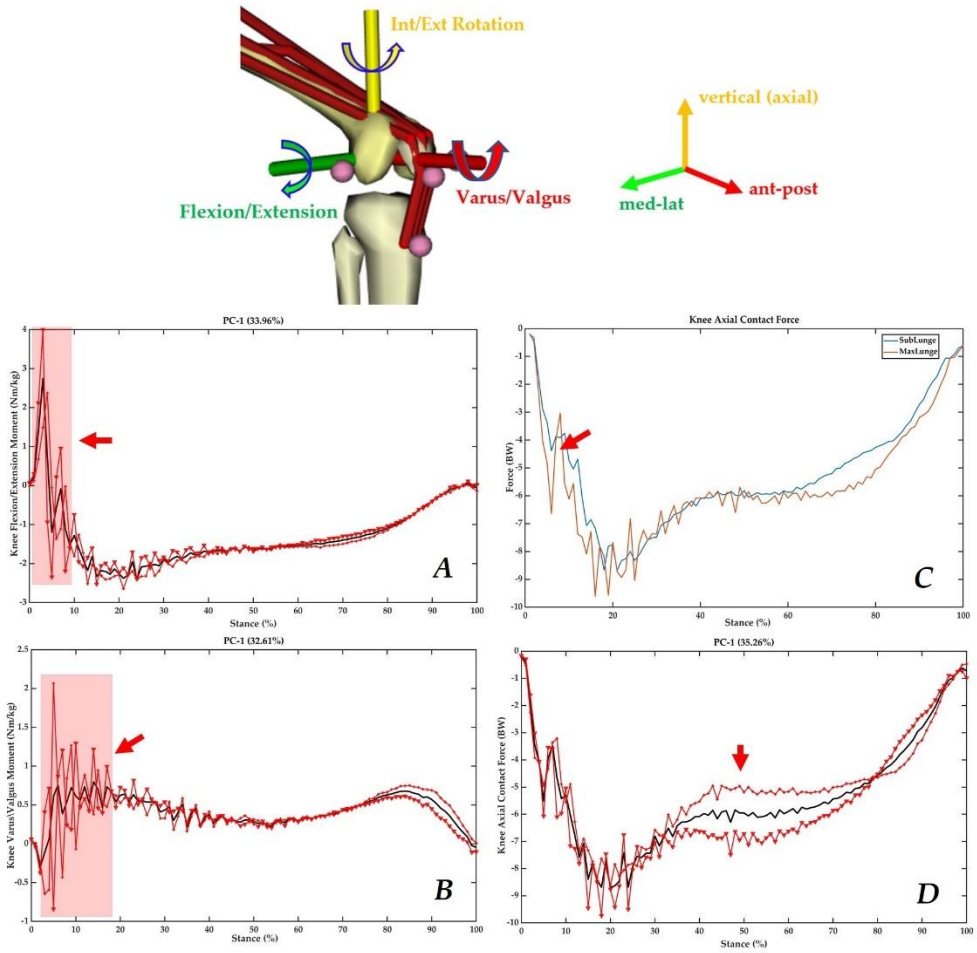

Figure 7. Principal mode of knee moments variation (**A & B**), and mean and principal variation in the axial knee contact force (**C & D**)

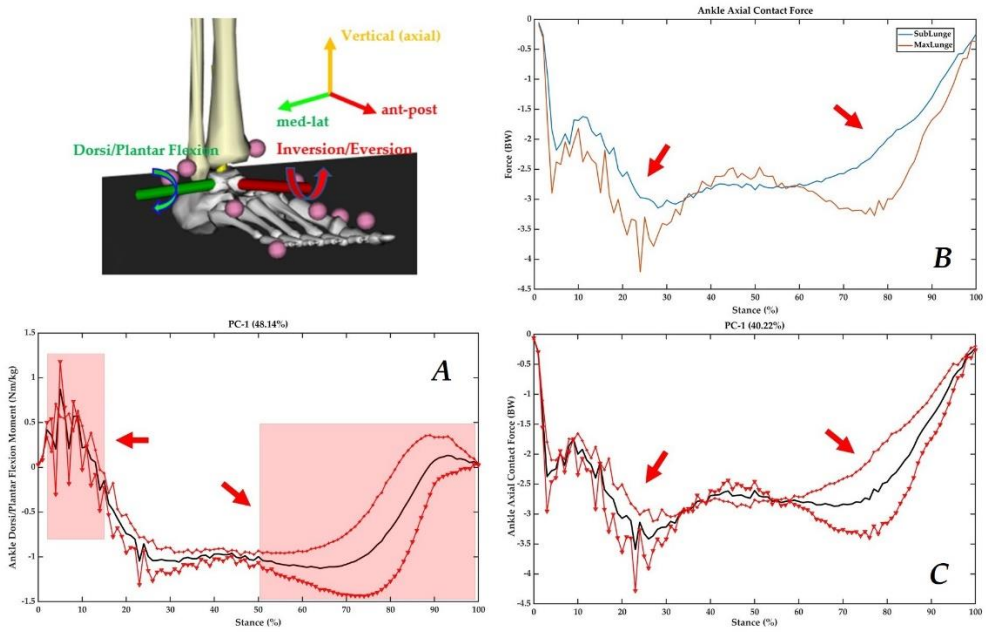

Figure 8. Principal variation of ankle dorsi/plantar flexion moment (**A**), and mean (**B**) and principal mode of ankle axial contact force (**C**)

3.2 PLSR

Following the PCA modelling, the ***LR*** (loading rate), peak ***knee*** flexion/extension, varus/valgus, and int/ext rotation ***moments***, peak ***ankle*** dorsi/plantar flexion, inver/eversion ***moments***, peak ***knee*** ant-post/med-lat/axial (vertical) ***contact forces***, and peak ***ankle*** ant-post/med-lat/axial (vertical) ***contact forces*** were used as loading parameters for responses in the PLSR machine learning model. Signals from IMU sensors, such as contact times, velocity, peak acceleration (knee) and peak acceleration (ankle), were input as predictors in the PLSR machine learning model.

Together with the four predictors, a prediction accuracy of 94.52% was observed for the moments and contact forces in the knee and ankle joints (**Figure 9**). To test the sensitivity of the peak knee and ankle acceleration, we performed a 'leave-one-out' cross validation and found that both peak knee and ankle acceleration could predict 93.72% of the loadings. Specifically, the knee peak acceleration had an 88.76% of prediction accuracy and the ankle peak acceleration had a 93% of prediction accuracy.

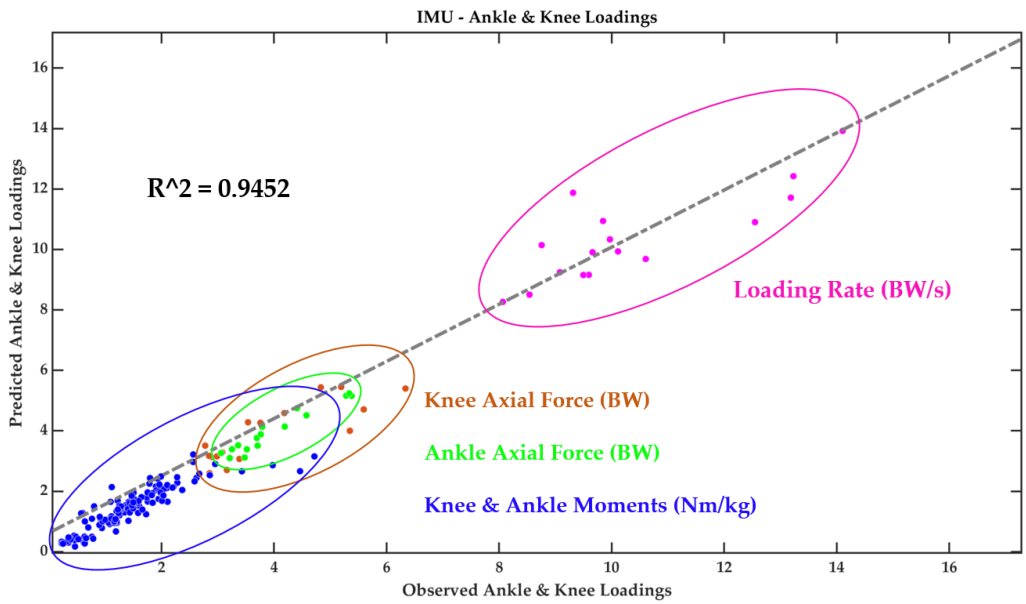

Figure 9. Performance of the PLSR machine learning model

4. Discussion / Implications

This project firstly integrated the wearable sensors with in-lab motion capture analysis to correlate the data from wearables, aiming to develop and validate machine learning prediction models. Secondly, wearable sensors were

attached on badminton athletes' lower limb during training and/or competition for the on court 'real world' data collection. As the key findings indicated, the variances between the vertical GRF of sub- lunges and maximal- lunges located in the initial and secondary impact peaks (including the loading rate). Similar variances in the knee flexion/extension and varus/valgus moments were found in the time frames, apart from the axial knee contact force differed during the mid-stance. While the ankle dorsi/plantar flexion moment and axial contact force showed greater variances during the initial landing (impact absorption) and push off phases between sub- and maximal- lunges.

During the gait test, we employed the well-established protocols (Huang et al., 2014; Kuntze et al., 2010; W. K. Lam et al., 2017; Lin et al., 2015; Mei et al., 2017) for the motion capture and synchronously integrated the IMU sensors to set up ground truth 'gold-standard'. The wearable technologies have been implemented in the recognition of badminton relevant movements for game analysis, showing promising accuracy (Steels et al., 2020). The primary objectives of this project were to monitor the loadings (joint moments and contact forces) in the knee and ankle with machine learning models.

As for the injuries in the lower extremity of badminton players, several recent review studies on badminton injuries and lunges (W. Lam et al., 2020; Lee & Loh, 2019; Phomsoupha & Laffaye, 2020) reported that fatigue of musculature system was a key factor contributing to reduced performance and loading accumulation (increased injury risks). Dynamic loading accumulation and distribution in the 'real world' scenario data from wearables during training and competition were monitored and reported based on the correlative prediction machine learning model. Typically, it was demonstrated that an physics-based and machine learning combined model offered promising solutions for tibia loading accumulation (Matijevich et al., 2020).

The main features extracted from PCA modelling in the vertical GRF and knee and ankle moments and contact forces were the magnitude difference, considering that the occurring of different timeframe during stance. Specifically, during the initial and secondary impact peak phases, the variances in the knee and ankle moments were observed, which may be explained by the different approaching speeds between sub- (~2,5m/s) and maximal- (~3.5m/s) lunges, similar to recent studies (Chen et al., 2020; W. K. Lam et al., 2018). Whilst the axial knee contact force varied between sub- and maximal- lunges during mid-stance of weight acceptance phase, which may be attributed to higher impact

and highly activated muscular contractions. The difference between directional lunges were not reported as being studied in our previous project that left-side (backhand) forward and backward lunges showed higher knee loadings than the right-side lunges. This was aimed to mimic the real on-court situation that shuttles were not returned in an anticipated manner from the opponent, and athletes could perform any directional lunges.

In terms of the difference during drive off in the ankle plantarflexion moment and axial contact forces, these may be the different multi-joint coordination patterns, as higher motion acceleration and deceleration could be observed in the sub- and maximal- lunges (Lee & Loh, 2019). The different acceleration and deceleration strategies or coordination thus exerted greater impact in the ankle, which functioned as the primary interface with the court.

The multivariate machine learning (PLSR) model we developed showed promising performance (~94.52% accuracy) while input the contact times, approaching velocity, peak ankle acceleration and knee acceleration to predict knee and ankle loadings. These input parameters could be easily measured or calculated from the IMU sensors. In order to simplify the machine learning prediction model, we trained the PLSR model with peak ankle and knee acceleration, showing similar accuracy (~93.72%). Considering the attachment of two belts with IMU to the proximal and distal tibia may limit the movements of badminton athletes, we used the single knee or ankle IMU each as predictor in the PLSR model, and the knee IMU and ankle IMU showed accuracy of 88.76% and 93%, respectively. From the sensitivity analysis of the PLSR model we developed, it was learnt that a single IMU sensor attaching to the anterior distal tibia above the medial malleoli could predict approximately 93% of loadings in the ankle and knee joint. Meanwhile, the 15% of total step accounts measured during one single match could be used to estimate the loading accumulation in the knee and ankle joints.

In summary, this project utilized the wearable technology and machine learning models to assist monitoring of joint loadings from lab to on-court 'real-world' scenario. The intelligent and dynamic framework developed in the current project provide a perspective to address the gap between lab and court analysis. The intelligent monitoring and feedback of loading patterns or accumulation would be integrated to design the training and competition schemes in a scientific manner, thus help prevent fatigue, reduce potential loading-accumulation related injury and maximize athletic performance.

5. Appendix – Machine learning models

The appendix includes PCA (principal component analysis) modelling of vGRF (vertical ground reaction force), moments and contact forces in the knee and ankle joints.

5.1 Appendix I – Principal Component Analysis (PCA) Model (feature extraction)

```
% Principal Components Analysis (PCA) modelling of vGRF, Moments and Contact forces
% Qichang Mei, Nov 2020, Ningbo University; The University of Auckland
% Email: qmei907@aucklandui.ac.nz

clear; clc   %clear workspace
close all    %close all figures


%% Load and combine data into a single array
 load('sub_max_lungeGRFv.mat');
 Y = [sub_lunge max_lunge]';
 t = linspace(0, 100, 101)';  %time


%% Run PCA
[coeff,score,latent,tsquared,explained] = pca(Y);

%% Visualize mean of sub and max lunges
figure (1)
plot (mean(sub_lunge'), 'linewidth', 2);
hold on
plot (mean(max_lunge'), 'linewidth', 2);
legend ('SubLunge', 'MaxLunge')

%% Visualize first two PCs
figure(2)
pc1 = coeff(:,1);
pc2 = coeff(:,2);
pc3 = coeff(:,3);
plot(t, pc1, 'r', 'linewidth', 3)
hold on
plot(t, pc2, '--k', 'linewidth', 3)
hold on
plot(t, pc3, ':b', 'linewidth', 3)
legend('PC-1', 'PC-2', 'PC-3')


%% Visualize first PC in the context of the overall mean trajectory
figure(3)
ymean = mean(Y, 1)';
scoresd = std(score, [], 1)';
plot(t, ymean, 'k', 'linewidth', 3)
hold on
plot(t, ymean + scoresd(1) .* pc1, '-r+', 'linewidth', 2)
plot(t, ymean - scoresd(1) .* pc1, '-rv', 'linewidth', 2)
title('PC-1')


%% Visualize second PC in the context of the overall mean trajectory
figure(4)
plot(t, ymean, 'k', 'linewidth', 3)
hold on
```

```
plot(t, ymean + scoresd(2) .* pc2, '-k+', 'linewidth', 2)
plot(t, ymean - scoresd(2) .* pc2, '-kv', 'linewidth', 2)
title('PC-2')

%% Visualize third PC in the context of the overall mean trajectory
figure(5)
plot(t, ymean, 'k', 'linewidth', 3)
hold on
plot(t, ymean + scoresd(3) .* pc3, '-b+', 'linewidth', 2)
plot(t, ymean - scoresd(3) .* pc3, '-bv', 'linewidth', 2)
title('PC-3')


%% Visualize first two PC scores
figure(6)
plot( score(1:8,1), score(1:8,2), 'bo' );
hold on
plot( score(9:16,1), score(9:16,2), 'ro' );
% plot( score(11:20,1), score(11:20,2), 'ro' );
xlabel('PC-1')
ylabel('PC-2')
legend('SubLunge', 'MaxLunge')
ax = gca();
plot([0 0], get(ax,'ylim'), 'k:')
plot(get(ax,'xlim'), [0 0], 'k:')

%% Visualize percentage explained and Accumulation
figure(7)
bar (explained (1:12, 1));
hold on
plot(cumsum(explained(1:12,1)), 'linewidth', 3)
xlabel ('PCs')
ylabel ('Variation Explained')
```

5.2 Appendix II – Partial Least Squares Regression (PLSR) Model (multivariate prediction)

```
% PLSR foot shape/pressure modelling in Matlab
% Qichang Mei, Nov 2020, Ningbo University & The University of Auckland
% Email: qmei907@aucklanduni.ac.nz


%% Read in data from an excel file.
% x are the predictors
% y are the responses

x = xlsread('IMU2GRF_Moment_ContactForce.xlsx','Sheet1','C3:F50');
y = xlsread('IMU2GRF_Moment_ContactForce.xlsx','Sheet1','I3:T50');


%% Create a PLSR model with 4 components
[Xloadings,Yloadings,Xscores,Yscores,betaPLS4,PLSPctVar] = plsregress(x,y,4);


% Create predicted output from PLSR model
[n,p] = size(x);
yfitPLS4 = [ones(n,1) x]*betaPLS4;
 plot(y,yfitPLS4,'bo','MarkerSize',8,'MarkerEdgeColor',[1 1 1],'MarkerFaceColor','b'); % Feel free to change MarkerSize,
MarkerColor, FontSize ... as your preferrence
 xlabel('Observed Ankle-Knee Loadings','FontSize',12,'FontWeight','bold');
 ylabel('Predicted Ankle-Knee Loadings','FontSize',12,'FontWeight','bold');
 title("IMU2Ankle-Knee Loadings","FontSize",16,'FontWeight','bold');


%% Compute RMSE value
RMSE = sqrt(mean((yfitPLS4 - y).^2));


%% Compute R2 value using corrcoef function (Prediction accuracy)
R=corrcoef(y,yfitPLS4);
Rsquared = R(1,2)*R(1,2)


%% Add line of best fit
 hold on;
   coef_fit = polyfit(y,yfitPLS4,1);
   y_fit = polyval(coef_fit,xlim);
   plot(xlim,y_fit,'-b','LineWidth',3);
  % display R2 value on plot at coordinates 1200,1200
  % text(10, 10, ['R^2 =' num2str(Rsquared)])
 hold off;
```

Reference

Chard, M. D., & Lachmann, S. M. (1987). Racquet sports--patterns of injury presenting to a sports injury clinic. *British Journal of Sports Medicine*, *21*(4), 150–153. https://doi.org/10.1136/bjsm.21.4.150

Chen, T. L. W., Wang, Y., Wong, D. W. C., Lam, W. K., & Zhang, M. (2020). Joint contact force and movement deceleration among badminton forward lunges: a musculoskeletal modelling study. *Sports Biomechanics*, *00*(00), 1–13. https://doi.org/10.1080/14763141.2020.1749720

Delp, S. L., Anderson, F. C., Arnold, A. S., Loan, P., Habib, A., John, C. T., Guendelman, E., & Thelen, D. G. (2007). OpenSim: Open-source software to create and analyze dynamic simulations of movement. *IEEE Transactions on Biomedical Engineering*, *54*(11), 1940–1950. https://doi.org/10.1109/TBME.2007.901024

Deluzio, K. J., Wyss, U. P., Zee, B., Costigan, P. A., & Sorbie, C. (1997). Principal component models of knee kinematics and kinetics: Normal vs. pathological gait patterns. *Human Movement Science*, *16*(2–3), 201–217. https://doi.org/10.1016/S0167-9457(96)00051-6

Fahlström, M., Björnstig, U., & Lorentzon, R. (1998). Acute badminton injuries. *Scandinavian Journal of Medicine and Science in Sports*, *8*(3), 145–148. https://doi.org/10.1111/j.1600-0838.1998.tb00184.x

Fong, D. T.-P., Hong, Y., Chan, L.-K., Yung, P. S.-H., & Chan, K.-M. (2007). A systematic review on ankle injury and ankle sprain in sports. *Sports Medicine*, *37*(1), 73–94. https://doi.org/10.2165/00007256-200737010-00006

Goh, S., Ali, M., Mokhtar, A., & Mohamed, I. (2013). Injury risk predictors among student badminton players in a Malaysian national sports school: Preliminary study. *Journal of Science and Medicine in Sport*, *16*, e59. https://doi.org/10.1016/j.jsams.2013.10.140

Huang, M.-T., Lee, H.-H., Lin, C.-F., Tsai, Y.-J., & Liao, J.-C. (2014). How does knee pain affect trunk and knee motion during badminton forehand lunges? *Journal of Sports Sciences*, *32*(7), 690–700. https://doi.org/10.1080/02640414.2013.848998

Jérgensen, U., & Winge, S. (1987). Epidemiology of Badminton injuries. *International Journal of Sports Medicine*, *8*, 379–382. https://doi.org/10.1136/bjsm.24.3.169

Kroner, K., Schmidt, S. A., Nielsen, A. B., Yde, J., Jakobsen, B. W., Moller-Madsen, B., & Jensen, J. (1990). Badminton injuries. *British Journal of Sports Medicine*, *24*(3), 169–172.

Kuntze, G., Mansfield, N., & Sellers, W. (2010). A biomechanical analysis of common lunge tasks in badminton. *Journal of Sports Sciences*, *28*(2), 183–191. https://doi.org/10.1080/02640410903428533

Lam, W. K., Ding, R., & Qu, Y. (2017). Ground reaction forces and knee kinetics during single and repeated badminton lunges. *Journal of Sports Sciences*, *35*(6), 587–592. https://doi.org/10.1080/02640414.2016.1180420

Lam, W. K., Lee, K. K., Park, S. K., Ryue, J., Yoon, S. H., & Ryu, J. (2018). Understanding the impact loading characteristics of a badminton lunge among badminton players. *PLoS ONE*, *13*(10), e205800. https://doi.org/10.1371/journal.pone.0205800

Lam, W., Wong, D. W., & Lee, W. C. (2020). Biomechanics of lower limb in badminton lunge: a systematic scoping review. *PeerJ*, *8*, e10300. https://doi.org/10.7717/peerj.10300

Lee, J. J. J., & Loh, W. P. (2019). A state-of-the-art review on badminton lunge attributes. *Computers in Biology and Medicine*, *108*, 213–222. https://doi.org/10.1016/j.compbiomed.2019.04.003

Lever, J., Krzywinski, M., & Altman, N. (2017). Points of Significance: Principal component analysis. *Nature Methods*, *14*(7), 641–642. https://doi.org/10.1038/nmeth.4346

Lin, C.-F., Hua, S.-H., Huang, M.-T., Lee, H.-H., & Liao, J.-C. (2015). Biomechanical analysis of knee and trunk in badminton players with and without knee pain during backhand diagonal lunges. *Journal of Sports Sciences*, *33*(14), 1429–1439. https://doi.org/10.1080/02640414.2014.990492

Matijevich, E. S., Scott, L. R., Volgyesi, P., Derry, K. H., & Zelik, K. E. (2020). Combining wearable sensor signals, machine learning and biomechanics to estimate tibial bone force and damage during running. *Human Movement Science*, *74*, 102690. https://doi.org/10.1016/j.humov.2020.102690

Mei, Q., Gu, Y., Fu, F., & Fernandez, J. (2017). A biomechanical investigation of right-forward lunging step among badminton players. *Journal of Sports Sciences*, *35*(5), 457–462. https://doi.org/10.1080/02640414.2016.1172723

Phinyomark, A., Petri, G., Ibáñez-Marcelo, E., Osis, S. T., & Ferber, R. (2018). Analysis of Big Data in Gait Biomechanics: Current Trends and Future Directions. *Journal of Medical and Biological Engineering*, *38*(2), 244–260. https://doi.org/10.1007/s40846-017-0297-2

Phomsoupha, M., & Laffaye, G. (2020). Injuries in badminton: A review. *Science and Sports*, *35*(4), 189–199. https://doi.org/10.1016/j.scispo.2020.01.002

Rajagopal, A., Dembia, C. L., DeMers, M. S., Delp, D. D., Hicks, J. L., & Delp, S.

L. (2016). Full-Body Musculoskeletal Model for Muscle-Driven Simulation of Human Gait. *IEEE Transactions on Biomedical Engineering*, *63*(10), 2068–2079. https://doi.org/10.1109/TBME.2016.2586891

Reeves, J., Hume, P., Gianotti, S., Wilson, B., & Ikeda, E. (2015). A Retrospective Review from 2006 to 2011 of Lower Extremity Injuries in Badminton in New Zealand. *Sports*, *3*(2), 77–86. https://doi.org/10.3390/sports3020077

Rice, H., Weir, G., Trudeau, M. B., Meardon, S., Derrick, T., & Hamill, J. (2019). Estimating Tibial Stress throughout the Duration of a Treadmill Run. *Medicine and Science in Sports and Exercise*, *51*(11), 2257–2264. https://doi.org/10.1249/MSS.0000000000002039

Shahabpoor, E., & Pavic, A. (2017). Measurement of walking ground reactions in real-life environments: A systematic review of techniques and technologies. *Sensors (Switzerland)*, *17*, 2085. https://doi.org/10.3390/s17092085

Sheerin, K. R., Besier, T. F., & Reid, D. (2020). The influence of running velocity on resultant tibial acceleration in runners. *Sports Biomechanics*, *19*(6), 750–760. https://doi.org/10.1080/14763141.2018.1546890

Steels, T., Van Herbruggen, B., Fontaine, J., De Pessemier, T., Plets, D., & Poorter, E. De. (2020). Badminton activity recognition using accelerometer data. *Sensors (Switzerland)*, *20*, 4685. https://doi.org/10.3390/s20174685

Tenforde, A. S., Hayano, T., Jamison, S. T., Outerleys, J., & Davis, I. S. (2020). Tibial Acceleration Measured from Wearable Sensors Is Associated with Loading Rates in Injured Runners. *PM and R*, *12*(7), 679–684. https://doi.org/10.1002/pmrj.12275

Ueberschär, O., Fleckenstein, D., Warschun, F., Kränzler, S., Walter, N., & Hoppe, M. W. (2019). Measuring biomechanical loads and asymmetries in junior elite long-distance runners through triaxial inertial sensors. *Sports Orthopaedics and Traumatology*, *35*(3), 296–308. https://doi.org/10.1016/j.orthtr.2019.06.001

Van Hooren, B., Goudsmit, J., Restrepo, J., & Vos, S. (2020). Real-time feedback by wearables in running: Current approaches, challenges and suggestions for improvements. *Journal of Sports Sciences*, *38*(2), 214–230. https://doi.org/10.1080/02640414.2019.1690960

Xiang, L., Mei, Q., Song, Y., Gao, Z., Fernandez, J., & Gu, Y. (2020). EFFECTS OF MINIMALIST FOOTWEAR ON THE LOWER LIMB LINEAR ACCELERATION AND ANGULAR VELOCITY DURING RUNNING. *38th International Society of Biomechanics in Sport Conference*, 72–75. https://commons.nmu.edu/isbs/vol38/iss1/20

BWF

寧波大學
NINGBO UNIVERSITY

THE UNIVERSITY OF AUCKLAND
Te Whare Wānanga o Tāmaki Makaurau
NEW ZEALAND